

# Application of remote sensing time series for characterizing interactions between the vegetation and hydro-geomorphology in the high-latitude arid region floodplains

X Ablat<sup>1,2</sup>, G H Liu<sup>1,3</sup>, Q S Liu<sup>1,3</sup>, and C Huang<sup>1</sup>

<sup>1</sup>State Key Laboratory of Resources and Environment Information System, Institute of Geographic Sciences and Natural Resources Research, Chinese Academy of Sciences, Beijing 100101, China

<sup>2</sup>University of Chinese Academy of Sciences, Beijing 100049, China

E-mail: liugh@reis.ac.cn; liuqs@reis.ac.cn

**Abstract.** Floodplain hydro-geomorphology is the major factor for vegetation growth and biomass. Characterizing interaction between the vegetation and hydro-geomorphology is essential to better understanding river ecosystems in arid regions. In this study, considering the various hydro-geomorphological dynamics of floodplains, the study area was divided into four functional zones and spatialized lateral variations of the floodplain fluvial disturbance intensity, sediment erosion and deposition process, moisture dynamics and vegetation growth condition through Landsat and daily Moderate Resolution Imaging Spectroradiometer (MODIS) time series between 2010-2015. And analyzed the various interactions between floodplain vegetation and hydro-geomorphology in different floodplain lateral zones. Results shows that the highest vegetation NDVI values (>0.4) are distributed in the regularly static floodplain area where characterized regular flood inundation and has moderate moisture ability. Vegetation NDVI values in the frequency inundation, wet and highly dynamic floodplain area are mainly less than 0.2. Results indicate that different hydro-geomorphological processes dominated in floodplains, therefore plants and hydro-geomorphology interact each other in different ways from river to floodplain margins. Using remote sensing time series can be better characterizing the different interactions between floodplain vegetation and hydro-geomorphology. This study can help to better management of river ecosystems in the arid region floodplains.

## 1. Introduction

Floodplains are the most biodiverse ecosystems in high-latitude arid regions [1]. Floodplain vegetation response to the hydro-geomorphology is directly related to the proper functioning of riparian ecosystems, which act as a transient corridor between aquatic and terrestrial ecosystems [2]. Highly dynamic wandering river floodplains are randomly affected by irregular river water disruption, whereas increases and decreases in water levels are not affected by temporal and spatial restrictions. Vegetation growth and biomass also change when the above factors vary [3]. High revisit rate remote-sensing images can be used to capture continuous rapid changes that occur in the vegetation, hydrology and geomorphology of floodplains [4].

Remote sensing is a useful tool for investigating spatial-temporal variations in floodplain dynamics



[5], providing a potential tool for quantifying the characteristics of floodplains in arid regions [6]. Because of their geographic location, dry floodplain regions have fewer cloudy days and a minimal tree canopy [7]. Remote sensing has a number of features, such as time-series records, high time resolution and easily acquired river landscape information that benefit to investigate the relationship between floodplain vegetation and hydro-geomorphology [8].

The objective of this study is to characterize the different interactions between vegetation and river hydro-geomorphology from the riverbed to floodplain margins. The most northern part and the highly dynamic wandering reach of the Yellow River was selected as a study reach. Different statistical indicators of a pixel-based time-series NDVI, LSWI and floodplain areas were used to characterizing the different zonal distribution patterns of the floodplain vegetation and hydro-geomorphology interactions. This result can provide useful information for the better management of river ecosystems in high-latitude arid regions.

## 2. Study reach and methods

### 2.1. Study reach

The study reach is located in the southwestern region of Inner Mongolia ( $107^{\circ} 24''$  E,  $40^{\circ} 38''$  N ~  $107^{\circ} 26''$  E,  $40^{\circ} 39''$  N) and the most northern part of the Yellow River (figure 1), and it presents a typical arid and semi-arid inner continental climate [9]. The yearly mean precipitation is 150-400 mm, and 75% of the precipitation is concentrated between June and September, summers are hot and dry, whereas winters are cold and long. The minimum winter temperature is  $-39^{\circ}\text{C}$  [10]. The floodplain has an area of  $500\text{ km}^2$ . The longest part of the floodplain is 30 km and the widest part is 5 km, is a typical wandering river floodplain. The vegetation types mainly consist of salt-tolerant vegetation, such as *Bermuda grass*, *Suaeda salsa*, and *Sporobolus virginicus*.

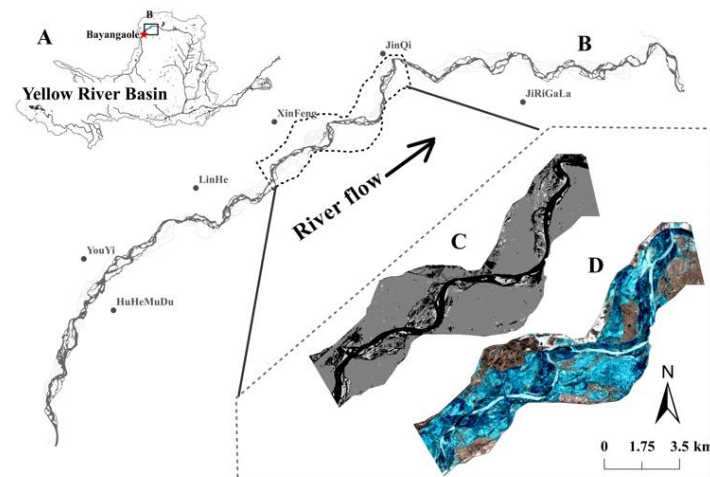


**Figure 1.** (A) The Yellow River Basin and location of the Linhe Reach (in black box); (B) The Linhe Reach and location of the study area (in dashed lined box); (C) NDVI image for the study reach in the 15 Aug. 2015. (D) False color composited image of Landsat 8 of the study area collect from 12 Jan. 2015

The geographical conditions and the direction of water flows from a low latitude to a high latitude, the freeze-up occurs from downstream to upstream in winter and break-up occurs from upstream to downstream in spring, which may let to ice jams or ice dams due to the quick increase in the ice-melt flood. the study reach occurs two times different degrees of the ice flooding phenomena in each year

[11]. These periods the study area presents a serious water banked-up phenomenon that occurs in the Yellow River during Nov to Apr in next.

The study reach is part of the Hangjinnaoer natural conservation area that is relatively unaffected by human activities, and vegetation productivity mainly depend on the floodplain hydro-geomorphological dynamics. Therefore, it considered a “natural laboratory” for investigating the changing floodplain dynamics of the Yellow River [12].

## 2.2. Zonal distribution concept of the study area

Highly dynamic wandering rivers are located in high latitude arid regions which presents more complex hydro-geomorphological dynamic activities that continuously affect floodplain vegetation productivity. Does the interactions between the floodplain vegetation and hydro-geomorphology are different from river to edge of floodplains? Before answer this question, we assume that the interactions between the floodplain vegetation and hydro-geomorphology will present significant spatial variations from the riverbed to floodplain margins. The study area is a main reach of the Upper Yellow River, where scouring and silting processes are quite complex [11]. In addition, the floodplains located in the high latitudes also experience the ice jamming phenomenon in each winter, which complicates floodplain hydrological processes. Therefore, we define four dynamic zones in river channels and their floodplains dominated by different hydro-geomorphological patterns and caused vegetation and hydro-geomorphological process interact with each other in different ways, including: (1) The highly dynamic continuously inundation zone is covered by water all year, is mainly submerged by deep water, has less vegetation growth, and high sediment dynamics characteristics. (2) The highly dynamic frequently inundation zone experiences dramatically changing water levels, is strongly affected by the river geomorphology, and has some vegetation that is influenced by changes in the summer and winter river water levels. Furthermore, the spatial distribution of the vegetation growth patterns is highly dynamic. (3) The static regularly flooded zone is affected by regular ice jams. Floodplain geomorphology is highly stable. Vegetation growth has distinct seasonal characteristics and presents a regular inter-annual contrast. (4) The static extremely rarely flooded zone includes floodplains that experience flooding less than once in 50 years, and the vegetation in this area relies on summer runoff and winter snow. Floodplain geomorphology is rarely interrupted by floodplain hydrology, and has relatively static geomorphological characteristics.

## 2.3. Data processing

### 2.3.1. MODIS images processing.

Daily Aqua/Terra Moderate Resolution Imaging Spectroradiometer surface reflectance bands 1-2 (MODIS9GQ) images with a spatial resolution of 250 m were downloaded in bulk from the Level-1 and Atmosphere Archive & Distribution System Distributed Active Archive Center (LAADS DAAS) at the Goddard Space Flight Center website [13] using Wget software [14]. A total of 8000 images with relevant tiles of H26V04 (horizontal number 26 and vertical number 04) were downloaded for 1 Jan. 2010 to 31 Dec. 2015. MODIS images used here have undergone standard corrections for gasses, aerosols and Rayleigh scattering; however imperfect corrections may affect results in using time series of remotely sensed images. Data were re-projected from the sinusoidal to the WGS84 geographic coordinate system, images were clipped by a study area vector border map, and image types were converted to Tag Image File format on the website before downloading. Subsequently, cloud-free images were selected from the post processed images. The Normalized Difference Vegetation Index (NDVI) has been used extensively to examine vegetation growth and biomass in arid floodplains [8]. Therefore, it can be used to investigate the vegetation responses to the river hydro-geomorphology in the study area. The formula for the NDVI is as follows:

$$NDVI = (NIR - RED) / (NIR + RED)$$

where NIR is the reflectance value of the MODIS 9GQ 2-band (841-876 nm) and RED is the MODIS

9QA 1-band (620-670 nm).

The NDVI values range from -1 to 1, with negative values corresponding to areas that are completely open water and positive values corresponding to areas covered by green vegetation [8]. Here, several NDVI statistical indicators were used to identify the vegetation growth and geomorphological dynamics of floodplains, including peak NDVI value and inundation water persistence time.

Maximum NDVI value is the main indicator statistics from the NDVI value, and the maximum NDVI value was used to describe the different zonal distribution of floodplain vegetations from the riverbed to floodplain margins. The formula is as follows:

$$P_{NM} = \text{Max} (P_{t1(\text{NDVI})}, P_{t2(\text{NDVI})}, P_{t3(\text{NDVI})}, \dots, P_{tn(\text{NDVI})})$$

where  $P_{NM}$  is the maximum NDVI value of pixel $_{(x,y)}$  in images,  $t$  is the collecting time of images, and  $n$  is the number of images.

Inundation water persistence time is used to spatialize and map ice jamming in the study area. This parameter can effectively describe the spatial distribution patterns of floodplain hydrology. The formula is as follows:

$$P_{WP} = \sum_{i=0}^n P_{(WP)} = \text{Sum} (P_{1(WP)} + P_{2(WP)} + P_{3(WP)} + \dots + P_{n(WP)})$$

where  $P_{WP}$  is the total water persistence days of each pixel in the images, and  $n$  is the number of days.

**2.3.2. Landsat images processing.** In this study, we considering the same water level in each year on images between 2010-2015 (total 72 scenes), choice different series of Landsat satellite images, separately TM4-5 and OLI 8 (Image Path/Row:129/032). All images were downloaded from United States Geological Survey Institution [15]. Pre-processing included layer stacking, clipping and mosaicking.

The Land Surface Water Index (LSWI) was used to differentiate between dry and wet regions. The formula for the LSWI is as follows:

$$\text{LSWI} = (\text{NIR} - \text{SWIR1}) / (\text{NIR} + \text{SWIR1})$$

where SWIR1 is the reflectance value of the Landsat band 5 (1550-1750 nm, shortwave infrared, (OLI8-band 6)) and NIR is the Landsat band 4 (760– 900 nm, NIR, (OLI8-band 5)).

#### 2.4. Quantifying zonal distribution concept

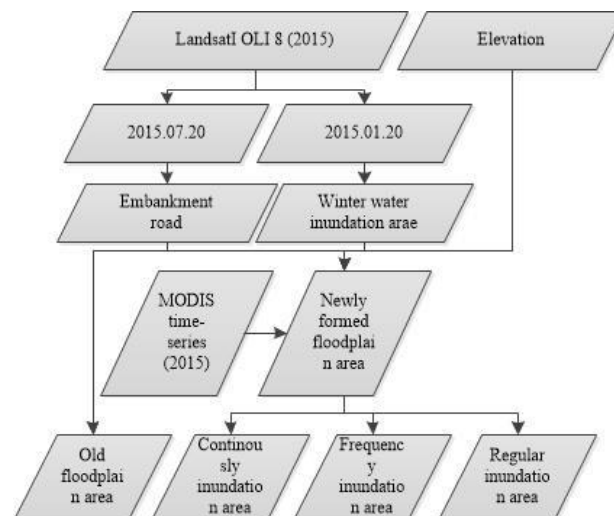


**Figure 2.** Flow chart of lateral zonal distributions in study area.

We combined elevation model and winter water inundation area from Landsat OLI summer (2015.1.20) and winter images (2015.1.20) along the embankment road divided entire study area into two parts: old floodplain area and newly formed floodplain area. Then based on the frequency of water persistence time statistics from daily MODIS-NDVI time series in 2015, the newly formed floodplain area was divided into continuously water inundation area, frequency water inundation area and regular static inundation area. At last, all study reach was divided into four lateral functional zones (figure 2), including: continuously water inundation zone (zone1), water frequency inundation zone (zone 2), regularly static floodplain zone (zone 3) and old floodplain zone (zone 4). Each indicator that mentioned in this paper statistics based on the above four regions (figure 3). Calculation methods as follows:

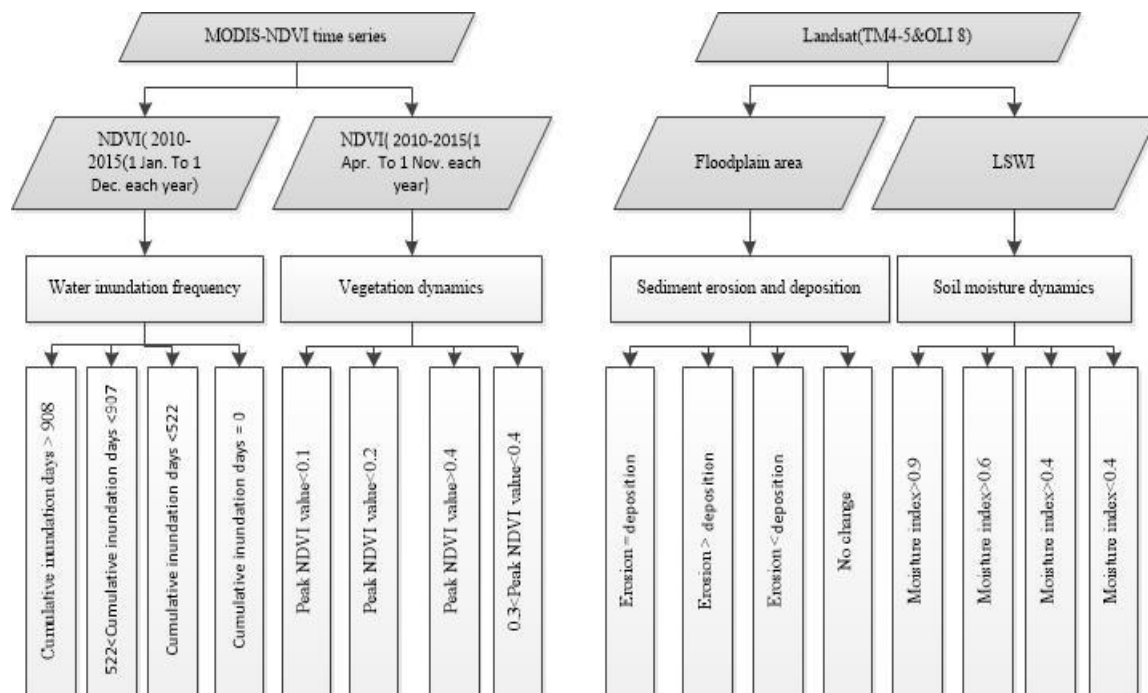


**Figure 3.** Simplified presentation of the work flow for conceptual model.

Maximum value calculation model in the ENVI software was used to acquired pixel-based peak NDVI images from daily MODIS-NDVI time series from 2010 to 2015 (from 1 Apr. to 1 Nov. in each year). And characterized different vegetation productivity in floodplain (figure 4A). Water persistence time was calculated through daily NDVI images from 2010 to 2015 (from 1 Jan. to 1 Dec. each year). At first, pixel-based daily water areas were extracted, then acquired to a floodplain water inundation persistence time map (figure 4C). Floodplain geomorphologic dynamics and moisture distribution patterns were acquired to Landsat images from 2010 to 2015. First, floodplain area was extracted in each year, then joined attributes of data in all study years and at last year by year comparison were conducted and acquired erosion and deposition area and moisture value in each year (figures 4B & 4D).

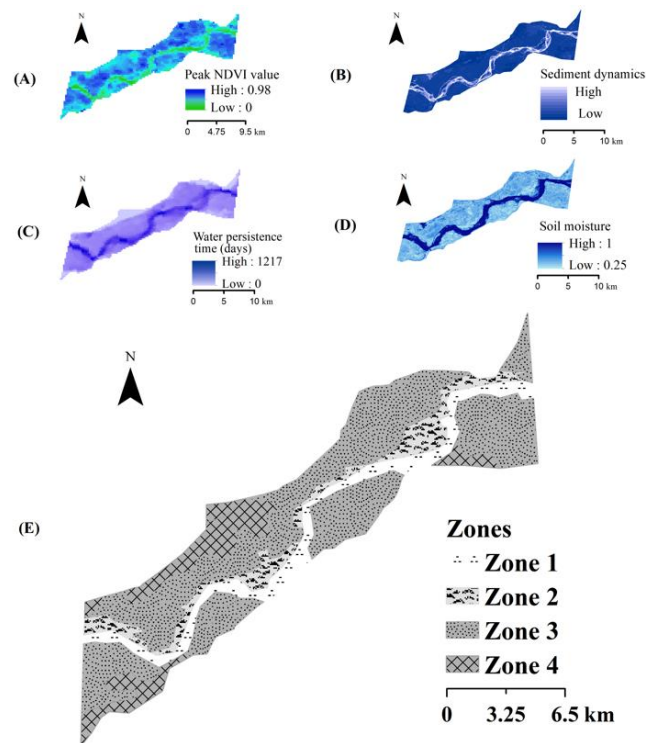


**Figure 4.** Zonal distribution patterns of the peak NDVI value (A), the sediment dynamics (B), the water persistence time (C) and the soil moisture distribution patterns (D) of the study area from 2010 to 2015. E is the different functional zones based on the hydrogeomorphological dynamics of study area.

### 3. Results

Water persistence times has significant zonal distribution characteristics, and the average water inundation persistence time of zones gradually decreases from the riverbed to edge of the floodplains. In the old floodplain zones, the persistence time of water inundation approximately 0 days. Inundation areas in the riverbed have a longest persistence time compared to other zones, and the persistence time larger than 908 days. Water inundation time of the newly formed static zone that located between the highest inundation frequency area and extremely rare inundation area, were ranging from 1 to 907 days.

Floodplain erosions in the highly frequency inundation area (zone 2) was approximately equal to the floodplain depositions. In the continuously inundation area (zone 1), floodplain erosions significantly higher than its depositions, in contrast, in newly formed static area, floodplain depositions higher than its erosions (zone 3), there are no significant changes in the extremely rare inundation zone in study periods (zone 4).

Highest soil moisture value occurred in continuously inundation zone that value between 0.9 -1. Soil moisture value from 0.6 to 0.9 mainly distributed in frequency inundation zone, in newly formed static area has moderate soil moisture compare to other zones, moisture value between 0.4 to 0. The moisture ability in old floodplain controlled by primary physical aspects and has lowest moisture values than other zones in study period.

The spatial distribution of the peak NDVI values in each different functional zone appeared to significant spatial distribution patterns. The peak NDVI values less than 0.2 were mainly distributed in the continuously and frequently inundation area (zone 1 and zone 2) whereas the highest peak NDVI values, which was greater than 0.4 emerged in the newly formed static floodplain area (zone 3). Peak

NDVI values in the old floodplain area (zone 4) were between 0.3 and 0.4, and this region presents an obvious border with the zone 3 that contains the highest peak NDVI values throughout the study reach (Fig.4A).

Strong lateral disturbances are attributable to frequency of inundation, associated flow velocities and surface shear stresses, and the mobilization, transport and deposition of sediments. These lateral disturbances change continually through time as river discharge varies and water spreads from the river channel into the river corridor. As a result, a lateral gradient in plant species and vigour should be expected at the reach scale, which vary laterally from riverbed to margin areas of floodplain areas. Regular water inundation static floodplain zone has been a good vegetation vigour and biomass. Water inundation times of the frequency inundation zone and extremely rare water inundation zone indicates that water inundation frequency too fast or too slow also disadvantage to vegetation growth and biomass, shows that vegetation growth and biomass were mainly controlled by the floodplain hydro-geomorphology. As a result lead to different interactions between the vegetation and hydro-geomorphological dynamics in different functional zones.

#### 4. Conclusion

Interaction between the floodplain vegetation and hydro-geomorphology is very essential for river ecosystem management in arid regions. In this study, we used pixel-based remote sensing time series, spatialized the floodplain water inundation frequency, vegetation productivity, soil moisture ability and sediment erosion and deposition conditions from 2010-2015. And through the different distribution patterns of each factors from river bed to the margins of floodplains, analyzed various interactions patterns between vegetation and hydro-geomorphology in different functional lateral zones. Results indicates that different hydro-geomorphological process dominate in floodplains, therefore plants and hydro-geomorphological process interact in different ways from river to floodplain margins. This study can help to better management of river ecosystems in high- latitude arid region floodplains.

#### References

- [1] Tockner K and Stanford J A 2002 Riverine flood plains: present state and future trends *Environ. Conserv.* **29** 308-30
- [2] Mohammadi A, Costelloe J F and Ryu D 2017 Application of time series of remotely sensed normalized difference water, vegetation and moisture indices in characterizing flood dynamics of large-scale arid zone floodplains *Remote Sens. Environ.* **190** 70-82
- [3] Riis T and Biggs B J F 2003 Hydrologic and hydraulic control of macrophyte establishment and performance in streams *Limnol. Oceanogr.* **48** 1488-97
- [4] Landmann T, Schramm M, Colditz R R, Dietz A and Dech S 2010 Wide area wetland mapping in semi-arid Africa using 250-meter MODIS metrics and topographic variables *Remote Sens.* **2** 1751-66
- [5] Sakamoto T, Van Nguyen N, Kotera A, Ohno H, Ishitsuka N and Yokozawa M 2007 Detecting temporal changes in the extent of annual flooding within the Cambodia and the Vietnamese Mekong Delta from MODIS time-series imagery *Remote Sens Environ* **109** 295-313
- [6] Haas E M, Bartholome E and Combal B 2009 Time series analysis of optical remote sensing data for the mapping of temporary surface water bodies in sub-Saharan western *Africa J. Hydrol.* **370** 52-63
- [7] Capon S J 2003 Plant community responses to wetting and drying in a large arid floodplain *River Res. Appl.* **19** 509-20
- [8] Marchetti Z Y, Latrubesse E M, Pereira M S and Ramonell C G 2013 Vegetation and its relationship with geomorphologic units in the Parana River floodplain, Argentina *J. S. Am. Earth Sci.* **46** 122-36
- [9] Wu J, Zhao L, Huang J, Yang J, Vincent B, Bouarfa S and Vidal A 2009 On the effectiveness of dry drainage in soil salinity control Science in China *Series E-Technological Sciences* **52**

3328-34

- [10] Su T, Wang S, Mei Y and Shao W 2015 Comparison of channel geometry changes in Inner Mongolian reach of the Yellow River before and after joint operation of large upstream reservoirs *J. Geogr. Sci.* **25** 930-42
- [11] Luo D, Mao W X and Sun H F 2017 Risk assessment and analysis of ice disaster in Ning-Meng reach of the Yellow River based on a two-phased intelligent model under grey information environment *Nat. Hazards* **88** 591-610
- [12] Peng J, Jia J L, Hu Y N, Tian L and Li H L 2018 Construction of ecological security pattern in the agro-pastoral ecotone based on surface humid index: A case study of Hangjin Banner, Inner Mongolia Autonomous Region, China *J. Appl. Ecol.* **29** 1990-8
- [13] Goddard Space Flight Center website available at: <https://labsweb.modaps.eosdis.nasa.gov>
- [14] Wget software download website available at: <https://eternallybored.org/misc/wget/>
- [15] United States Geological Survey Institution available at: <http://glovis.usgs.gov/>



Reproduced with permission of copyright owner. Further reproduction prohibited without permission.